Journal of Engineering Science and Technology
Vol. 21, No. 2 (2026) 480 - 494

MORPHOLOGICAL AND MECHANICAL ENHANCEMENT OF SAND PROPPANTS USING POLYURETHANE-BASED CARBON NANOTUBE NANOCOATING

ZAHRAA A. HAJOOL, ALI S. MUHSAN*, MUHAMMAD S. NASIF

Department of Mechanical Engineering, Universiti Teknologi PETRONAS (UTP), 32610 Bandar Seri Iskandar, Perak, Malaysia
*Corresponding Author: ali.samer@utp.edu.my

Abstract

Proppant performance plays a decisive role in sustaining fracture conductivity during hydraulic fracturing. Conventional sand, while inexpensive, exhibits poor sphericity, low mechanical strength, and severe fines generation, whereas ceramic and conventional resin-coated proppants, though more durable, remain costly and less widely applicable. This laboratory-scale study introduces a polyurethane-based nanocoating reinforced with carbon nanotubes (PU-CNT) as a scalable alternative to overcome these limitations. In this laboratory-scale study, sand proppants were coated with a polyurethane-carbon nanotube (PU-CNT) nanocomposite prepared via probe sonication and applied using a spray-coating technique. The nanocoated sand proppants exhibited notable morphological improvements, with sphericity and roundness increasing from 0.47 to 0.73 and 0.13 to 0.30, respectively. Surface wettability shifted from strongly hydrophilic 12° to hydrophobic 92°, enhancing hydrocarbon mobility. Mechanical testing confirmed superior crush resistance with fines generation reduced to 0.34%, significantly outperforming uncoated and conventional resin-coated counterparts. These results highlight the originality and practical significance of PU-CNTs coated proppants, offering a balance of cost-effectiveness, durability, and performance compared with current industry options.

Keywords: Hydraulic fracturing, Resin-coated-proppant, Sand proppants, Sphericity and roundness,.

1. Introduction

Hydraulic fracturing [1] has emerged as a vital technology for unlocking hydrocarbon resources from unconventional and tight formations, playing a transformative role in global energy production [2-4]. By injecting high-pressure fluids into low-permeability reservoirs, the process creates fractures that must be held open using solid particles known as proppants. The effectiveness and sustainability of hydraulic fracturing are closely tied to the characteristics of these proppants particularly their shape, roundness, mechanical strength, and resistance to fines generation [5-7].

Proppants are commonly categorized into three main types: natural sand, resin-coated sand, and ceramic proppants. Ceramic proppants offer superior strength and thermal stability but are significantly more expensive and heavier, limiting their use in certain field applications. Resin-coated sands offer moderate improvement but still exhibit degradation and fines release over time, especially at elevated temperatures. Among commercially available proppants, natural sand remains the most used due to its cost-effectiveness and availability.

However, Its inherent irregular morphology and angular geometry often result in higher frictional resistance, poor flowability, and susceptibility to mechanical degradation [8-10]. These shortcomings contribute to excessive fines generation, reduction in fracture conductivity, and ultimately, a decline in reservoir performance [1, 12]. The morphology of proppants, specifically sphericity and roundness, play a fundamental role in influencing their flow through wellbores, packing efficiency within fractures, and resistance to crushing under high closure stresses [13-15]. Well-rounded, spherical proppants have been shown to offer lower inter-particle friction, improved transport behaviour, and more uniform stress distribution.

To overcome the limitations of uncoated sand, researchers have explored a variety of surface modification strategies, including polymeric coatings, to improve proppant durability, morphology, and wettability [16, 17]. Among these, polyurethane (PU) [18-20] has gained attention for its ability to balance mechanical enhancement with flexibility, enabling better particle integrity under pressure without compromising transport performance [21, 22]. Polyurethane coatings also offer opportunities to tune surface properties such as roughness and wettability key factors influencing capillary behaviour and hydrocarbon flow [22].

Despite these advancements, most studies to date have focused on improving the mechanical strength or crush resistance of coated proppants, with limited attention given to their morphological transformation particularly how coatings influence particle shape and roundness. These parameters are critically important, not only for optimizing proppant transport and packing but also for ensuring uniform fracture propagation and sustained conductivity [23, 24]. Furthermore, the combined effects of polymer coatings and nanomaterial reinforcement such as the inclusion of carbon nanotubes (CNTs) remain underexplored.

Field deployment of double-shell coated proppants (DSCP) confirmed reduced fines and improved pack stability under actual reservoir conditions [25]. Likewise, on-the-fly resin-coating control in producing wells demonstrated significant suppression of proppant flowback, with conductivity maintained over extended production periods [26]. Advanced numerical models, such as CFD-DEM simulations, have shown that resin-coated proppants form stable agglomerates that

resist washout, leading to lower mobilization losses compared to uncoated sand [27]. In addition, placement optimization models demonstrated enhanced fracture coverage and retained conductivity in wells treated with resin-coated sands. Other simulations and slot-fracture validations similarly confirm that coated proppants outperform uncoated counterparts under high closure [28].

With the increasing reliance on hydraulic fracturing to meet global energy demand and considering the substantial economic losses associated with proppant failure and fines migration, the development of advanced coated proppants with improved morphology and stability has become both a scientific priority and an industrial necessity. Therefore, this study investigates the development of CNT-reinforced polyurethane coatings impact on sand proppants, focusing on morphology, wettability, and mechanical integrity. Through high-resolution imaging, contact angle analysis, and crush resistance tests, we evaluate how nanocoating enhance particle sphericity, roundness, and durability, with the ultimate goal of advancing proppants for more efficient and sustainable hydraulic fracturing operations.

2. Materials and Methods

2.1. Materials

The sand proppant (30/60 mesh) used in this study was obtained from Kim Yuan Amang Sdn. Bhd., Malaysia. Polyurethane (PU) was supplied by Weifang Waterproof Materials Co., Ltd.

2.2. Methods

2.2.1. Sample preparation

The 30/60 mesh sand proppants were coated with a thin layer of nanocomposite polyurethane (PU) resin reinforced with 0.1 wt% carbon nanotubes (CNTs) as illustrated in Fig. 1. The nanocomposite resin was prepared by dispersing the nanofillers into the PU matrix using a probe sonicator for 50 minutes at an amplitude of 50% to ensure a homogeneous distribution of the nanoparticles. Subsequently, the prepared nanocomposite PU-CNTs was applied onto the sand proppants by using a spray-coating technique, enabling the formation of a thin, uniform layer with good coverage. The coated samples were cured at ambient conditions for 72 h to enhance interfacial bonding between the sand surface and the nanocomposite topcoat.

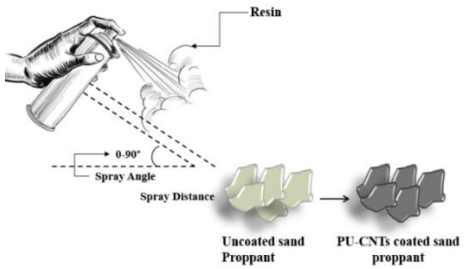

Fig. 1. Spray coating technique illustrating the application of PU-CNTs coating onto sand proppants.

2.2.2. Morphological analysis (SEM and optical microscopy)

The morphological characteristics of particles across various scale levels are crucial for interpreting the geological origin and mechanical behaviour of natural sands. Therefore, it is essential to characterize and quantify these features using a set of appropriate descriptors. The morphology and surface features of both coated and uncoated proppants were examined using a TESCAN VEGA Scanning Electron Microscope (SEM).

The coating thickness was measured with a Zeiss Supra 55VP Field Emission Scanning Electron Microscope (FESEM). To prevent charging artifacts and ensure high-quality imaging, the samples were sputter-coated with a thin gold layer for 30 seconds before examination.

2.3. Wettability analysis (contact angle measurement)

The wettability of the proppants was assessed using a contact angle goniometer, OCA 200. A water droplet was placed on the surface of coated and uncoated proppants [29, 30], and the contact angle was recorded. Wettability describes the relative affinity of a fluid to a solid surface and significantly influences fluid flow dynamics within porous media. This property is typically evaluated by measuring the contact angle (θ), which is defined at the point where the liquid-gas interface meets the solid-liquid interface. Based on the measured contact angle, surfaces are categorized as: Water-wet (hydrophilic) $\theta < 75°$, (hydrophobic) $\theta > 75°$. Understanding wettability is essential for optimizing fluid displacement and enhancing hydrocarbon recovery in fractured reservoirs [31-33].

2.4. Sphericity and roundness

To evaluate the variations in sphericity and roundness of the sand particles, micrographs of randomly selected samples were captured using a polarized scanning electron microscope (SEM). The particle shapes were assessed in accordance with the API RP 19C standard, employing the Krumbein–Sloss comparison chart as shown in Fig. 2.

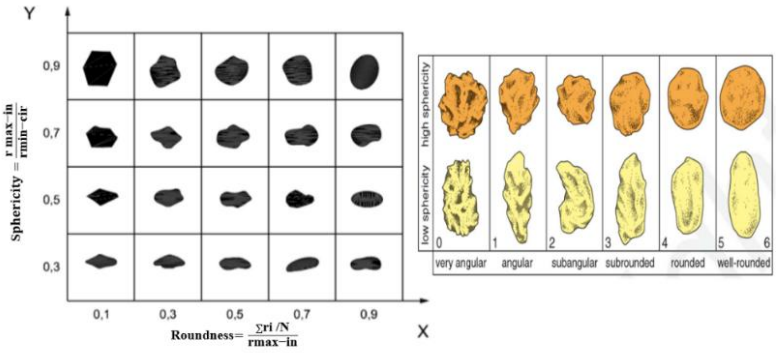

Fig. 2. Classification chart for particle shape evaluation based on sphericity and roundness. Adapted from Krumbein and Sloss [34] and illustrated by Cho et al. [35], and Zhou et al. [36].

Additionally, quantitative measurements of sphericity and roundness were performed using ImageJ software. The sphericity was determined as the ratio of the nominal particle diameter to the maximum intercept length across the particle:

$$\Psi = \frac{R_{max-in}}{R_{min-out}} \quad (1)$$

where R_{max-in} is the radius of the largest circle that can be inscribed entirely within the particle boundary (maximum inscribed radius), and $R_{min-out}$ is the radius of the smallest circle that can circumscribe the particle (minimum circumscribed radius). Roundness, on the other hand, was calculated as the mean radius of curvature of the particle corners:

$$Roundness = \frac{1}{n}\sum_{i=1}^{n}\frac{r_i}{R} \quad (2)$$

where n is the number of measured corners, r_i is the radii of curvature at distinct corners, and the mean value was normalized by the maximum inscribed radius is R.

2.5. Crushing resistance and Fines migration

The crush resistance test was performed to evaluate the mechanical durability of coated proppants under simulated hydraulic fracturing conditions, following the guidelines of ISO 13503-2 as shown in Fig. 3. A universal testing machine (UTM) was utilized for experiments.

During the test, the proppants were placed inside a steel crush cell and subjected to a gradual vertical load at a constant displacement rate of 1 mm/min. The applied load was steadily increased until it reached the target stress level of 100 kN, replicating the closure pressures typically encountered in hydraulic fractures. This method enabled the assessment of the structural integrity and compressive strength of the coated proppants under realistic field conditions.

The conductivity test was carried out to assess the impact of nanocomposite coatings on fracture conductivity, a key factor in sustaining hydrocarbon flow during hydraulic fracturing operations. A specially designed conductivity cell was employed to replicate the compressive forces that proppants experience within a fracture.

Throughout the test, the proppants were exposed to incrementally increasing compressive loads, while fracture conductivity was continuously monitored and recorded. This approach allowed for a systematic evaluation of how the coatings influence proppant performance under realistic operational conditions.

The migration of fine particles, generated during the crush resistance test, was analysed using a sieve analysis to quantify the amount of fines produced under compressive stress. Following the completion of the crush resistance test, the proppants were carefully retrieved from the steel crush cell and subjected to a sequential sieving process using mesh sizes of 500 μm, 300 μm, 150 μm and 38 μm, as depicted in Fig. 4. This methodology allowed for the segregation and classification of fine particles based on their size, providing valuable insights into their generation during compression.

The mass of particles passing through each sieve was recorded to determine the total amount of fines produced.

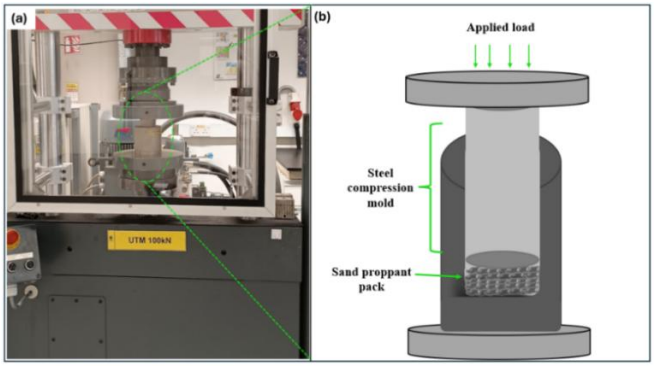

Fig. 3. UTM machine (100 kN) used for proppant crush resistance testing, following ISO 13503-2. (a) Actual setup; (b) schematic of sand proppant placement within the steel compression mold under axial load.

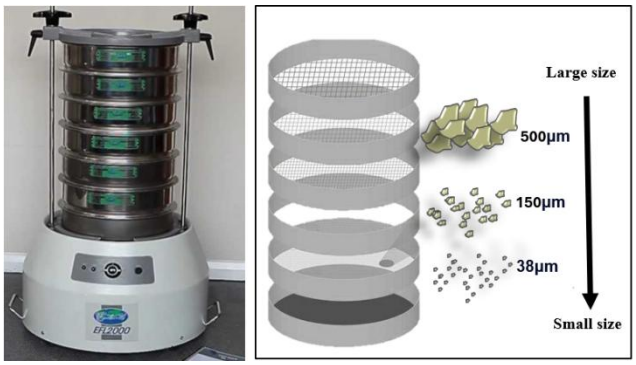

Fig. 4. Equipment and schematic for sieve-based particle size analysis.

2.6. Statistical analysis

All experiments were carried out in triplicate, and the results are presented as mean values with their corresponding standard deviations (SD) to ensure accuracy and reproducibility. Statistical comparisons between the coated and uncoated proppants were performed using the built-in analysis tools in OriginPro 2019 (OriginLab, USA). The software automatically calculated standard deviations and p-values from the replicate data to determine the significance of the observed differences. A confidence level of 95% ($p < 0.05$) was used to indicate statistical significance. All bar charts display error bars representing the SD, and significance letters were added where applicable to clearly illustrate meaningful differences among the various nanomaterial concentrations and coating types.

3. Results and Discussion

3.1. Morphological analysis

FESEM images in Fig. 5 illustrate the surface morphology and microstructural characteristics of the PU-CNT nanocoating on sand proppants at different magnifications. Figure 5(a) shows the overall coating layer conformally covering the sand grain, indicating good adhesion of the polyurethane-based nanocomposite to the

substrate. The magnified view in Fig. 5(b) reveals a more detailed surface texture, with a relatively uniform coating thickness of 872 nm, suggesting effective dispersion of the nanocomposite during the spray-coating process. Figure 5(c) provides high-resolution evidence of embedded carbon nanotubes (CNTs) within the polymeric matrix, where the CNTs are well integrated into the coating structure, creating a reinforcing network that enhances crack resistance and mechanical stability.

The presence of CNTs within the coating is particularly significant, as they act as nanoscale bridges that limit crack propagation, increase load transfer efficiency, and contribute to the suppression of fines generation under compressive stress. Collectively, the microstructural observations confirm that the PU-CNT nanocoating produces a dense, continuous, and reinforced protective layer on the sand surface, which underpins the improved morphological, mechanical, and durability properties of the coated proppants.

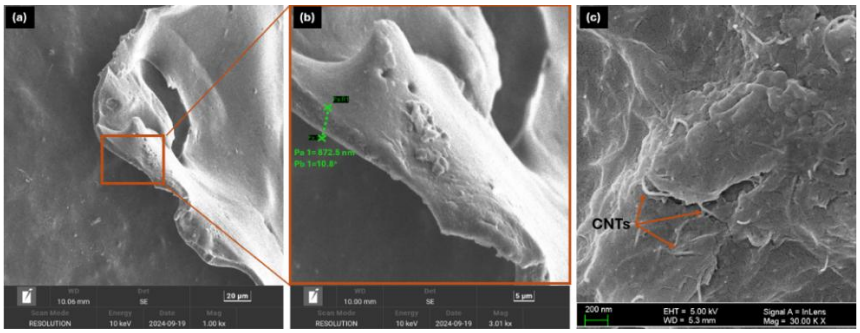

Fig. 5. FESEM images of a polyurethane-coated proppant particle at varying magnifications: (a) overall surface texture, (b) localized surface morphology, and (c) coating thickness measurement.

3.2. Sphericity and roundness

The sphericity and roundness of proppant particles are fundamental parameters that strongly influence their performance in hydraulic fracturing. Rounded particles facilitate uniform stress distribution, minimize crushing under closure stresses, and help preserve fracture conductivity over long production periods.

In this study, two representative particle types were analysed: uncoated sand and coated sand, to quantify their sphericity and roundness using Eqs. (1) and (2), followed by classification according to the Krumbein-Sloss (K-S) chart.

The geometric evaluation of the particles demonstrated that the coating had a clear effect on both sphericity and roundness. For the uncoated particles, the sphericity was measured at 0.47 and the roundness at 0.13, reflecting a relatively irregular morphology with sharp edges and poor conformity to a spherical shape. After coating, the sphericity increased to 0.73, while the roundness rose to 0.30. These results demonstrate that the coating process significantly improves particle shape, as illustrated in Fig. 6.

The increased roundness suggests that the coating process not only maintains the structural integrity of the particle but also contributes to smoother edges and reduced angularity, which are essential for minimizing flow resistance and

optimizing fracture conductivity, as summarized in Table 1. Figure 7 presents microscopic images comparing the surface morphology of uncoated and coated sand proppants. Figures 7(a) and (b) depict the uncoated proppant, which exhibits sharp edges, angular shapes, and a relatively rough surface texture indicative of its natural, unmodified state. In contrast, Figs. 7(c) and (d) display the coated proppant, where the particles appear smoother, with rounded edges and a glossy, more uniform surface. The coating significantly alters the particle morphology by filling in surface irregularities and reducing angularity, potentially enhancing flowability and reducing friction during proppant transport in hydraulic fracturing applications. These morphological changes are crucial for improving the mechanical performance and durability of the proppants under downhole conditions.

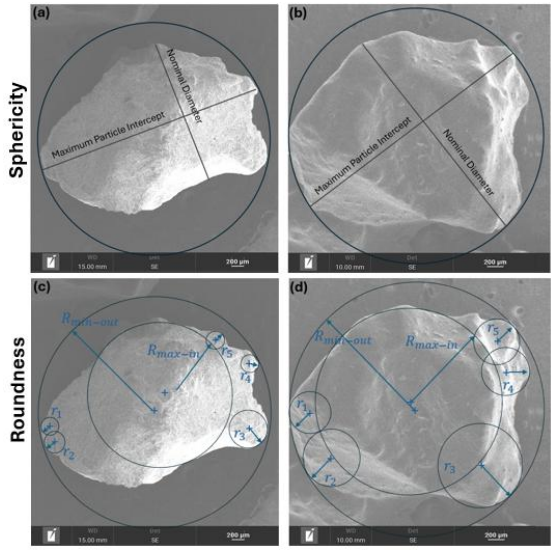

Fig. 6. SEM images of proppant particles with dimensional measurements: (a) coated proppant and (b) uncoated proppant, illustrating differences in surface texture and particle size.

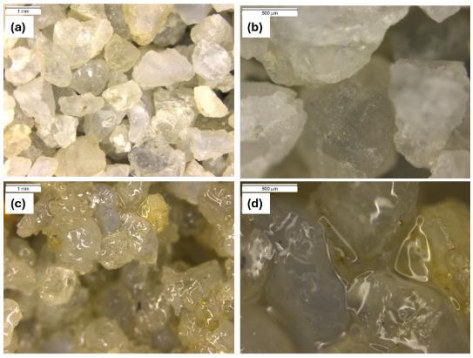

Fig. 7. Optical microscopy images comparing uncoated and coated sand proppants: (a, b) uncoated particles with angular morphology and rough surfaces; (c, d) coated particles exhibiting smoother, rounded surfaces due to polyurethane nanocoating.

Table 1. Comparison of sphericity and roundness improvements of sand proppants with different coating strategies from current and previous studies.

Proppant	Coating	Effect of (Sphericity/Roundness)	Ref.
Malaysian sand	PU-CNTs	Remarkable improvement in sphericity (0.47 chart; 0.73 ± 0.05 calc), and roundness (0.13; 0.3).	Our study
Malaysian sand	Graphene oxide (GO)-epoxy	Sphericity increased (0.8 chart; 0.70 ± 0.07 calc); low roundness (0.3; 0.27)	[37]
Sand, ceramic (Review)	Various polymeric resins	Coating enhances apparent sphericity and roundness variably	[38]
Sand/ceramics	Industry resin coatings	Resin smooths angular contact, reduces stress concentration	[38]
White sand	Nano-modified resin coatings	Sphericity/roundness > 0.6 post-treatment	[39]

3.3. Surface wettability analysis

The wettability of solid surfaces is assessed through contact angle measurements, which quantify the interaction between a liquid and a solid interface. Conventional silica sand proppants are naturally water-wet, typically displaying contact angles below 75°.

Figure 8 illustrates the contact angle measurements for different proppant types, including uncoated proppants and resin-coated proppants (RCP). The uncoated proppants (Fig. 8(a)) had a contact angle of 12°, confirming their strong hydrophilic properties, which are typical of silica-based proppants. In contrast, resin-coated proppants (RCP) (Fig. 8(b)) exhibited a contact angle of 85°, reflecting a shift toward a more neutral wetting behaviour due to the polyurethane coating. Furthermore, the incorporation of carbon nanotubes (CNTs) into the polyurethane coating further enhanced the surface hydrophobicity, increasing the contact angle to 92° as shown in (Fig. 8(c)).

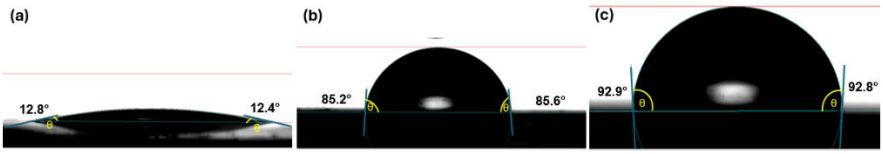

Fig. 8. Contact angle measurements showing wettability behaviour of (a) uncoated sand surface, (b) polyurethane-coated surface and (c) PU-CNTs coated surface.

The altered surface characteristics reduce capillary forces, thereby limiting water retention within the proppant pack and increase the hydrophobicity properties as shown in Table 2. By preventing water entrapment, these coatings enhance hydrocarbon mobility and promote more efficient fluid transport within fractured reservoirs.

Table 2. Wettability transition of uncoated, PU, and PU-CNTs coated proppants.

Proppant Type	Contact Angle	Remarks
Uncoated sand	12°	Hydrophilic surface, indicating strong water affinity and poor wettability control
Pu-resin coated sand	85°	Transition towards hydrophobic behaviour; coating improves wettability and fluid selectivity
Pu-CNTS coated sand	92°	Fully hydrophobic surface, enhancing hydrocarbon affinity and reducing water retention

3.4. Sand proppants fine migration

The sieve analysis results clearly demonstrate the significant influence of incorporating CNTs in polyurethane (PU) resin coating on fines generation compared to resin coated sand and uncoated sand, as shown in Table 3.

Table 3. Generated fines (%) for uncoated, PU-coated, and PU-CNTs-coated sand at different sieve sizes.

Sieve Size (µm)	Uncoated Sand (% ± SD)	PU Resin Coated Sand (% ± SD)	PU-CNT Coated Sand (% ± SD)
500	76.15 ± 0.48	30.43 ± 0.30	8.55 ± 0.21
150	18.63± 0.3	10.28 ± 0.22	2.04 ± 0.16
38	4.81±0.18	2.61 ± 0.13	0.34 ± 0.05

For uncoated sand exhibited the highest amount of crushed fragments retained across the sieve sizes, indicating severe particle breakage under compressive loading, as shown in Fig. 9. In contrast, the PU-resin-coated sand showed a considerable reduction in fines distribution, confirming the role of the polymer layer in enhancing grain strength and minimizing fragmentation. More notably, the PU–CNT–coated proppants exhibited the lowest fines generation among all samples, signifying the synergistic reinforcement effect of CNTs in improving coating toughness and resistance to crack propagation. The incorporation of CNTs within the PU matrix provides additional load-bearing pathways and restricts the detachment of small fragments, thereby reducing secondary fines release.

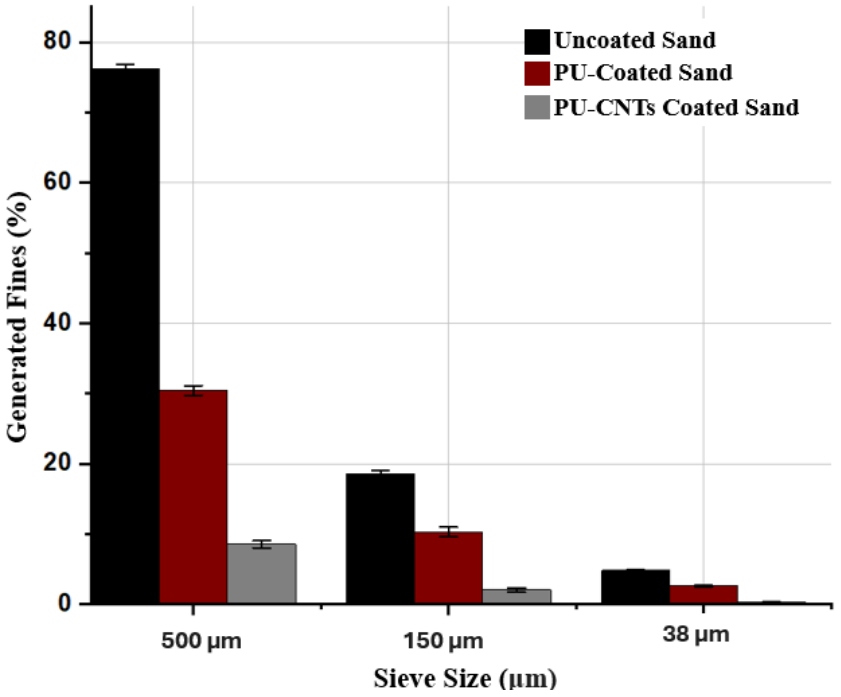

Fig. 9. Percentage of fines generated from coated and uncoated sand proppants after compression, categorized by sieve size (500 µm, 150 µm, and 38 µm).

Overall, the findings indicate that polyurethane reinforced with CNTs coatings play a crucial role in improving proppant performance by minimizing fines generation and migration as summarized in Table 4. This improvement is particularly advantageous in hydraulic fracturing operations, where minimizing fines migration helps maintain fracture conductivity and ensures stable hydrocarbon flow over extended production periods.

Table 4. Summary of mechanical performance and fines generation control of PU–CNT coated sand proppants compared with various proppant types reported in previous studies.

Proppant Type	Test Condition	Key Findings	Ref.
Pu-CNTS coating	Mechanical testing under compressive stress 100 kN	Coating reduces 1% less fines. Crush strength can range of 45 MPa.	Our study
Polymer-coated sand/Resin coating	Mechanical testing under compressive stress	Coating reduces 10% less fines. Crush strength can range from 2000 to 12,000 psi.	[40]
Various resin coatings, surface modifications	Laboratory evaluation of crush resistance, embedment, and fines content	Resin coatings effectively reduce fines and improve overall proppant durability.	[41]
Polymer-nanofiller composite coatings	Review of multiple lab-scale studies under high-stress fracturing conditions	Coatings reduce production of fines from 5% (neat PMMA) to 0.5% (PMMA-3 wt% SDS. modified graphite) at 69 MPa (10000 psi).	[41]
Microsand with dual polymer nanocomposite coating epoxy-CG	Thermo-mechanical analysis and high-stress load testing.	Coating reduces production fines less than 5% closure stress from 3000 psi to 14000 psi.	[42]
Ceramic proppants	Dry crush tests under final stress ~15,000–30,000 psi (≈103–207 MPa).	All ceramic samples, implying it yields less than 10 % of fines at 10,000 psi.	[43]

4. Conclusion

The present study has comprehensively demonstrated that polyurethane–carbon nanotube (PU-CNTs) nanocoatings can substantially enhance the overall performance of sand proppants intended for hydraulic fracturing applications. From a morphological perspective, the coating process produced a significant improvement in particle geometry, with sphericity increasing from 0.47 to 0.73 ± 0.05, and roundness rising from 0.13 to 0.30. These enhancements translate directly into improved packing efficiency and flowability within fracture networks, which are widely recognized as critical parameters for sustaining high fracture conductivity.

Surface modification through nanocoating also yielded a marked alteration in wettability. The contact angle shifted from a strongly hydrophilic 12° in uncoated sand to 92° in PU–CNT-coated proppants, indicating a transition to a distinctly hydrophobic character. Such a shift not only reduces water retention but also promotes preferential hydrocarbon transport, thereby improving reservoir stimulation efficiency.

Mechanical testing further highlighted the superior durability of the PU–CNT-coated proppants. Fines generation, a major concern in proppant performance,

decreased from 4.81% in uncoated sand to only 0.34% after PU–CNT nanocoating, representing more than a 90% reduction under stresses up to 45 MPa. Building on these findings, the developed PU–CNT–coated proppants exhibit strong potential for field implementation, particularly in enhancing fracture stability and reducing fines migration. The observed improvements in sphericity, roundness, and crush resistance indicate superior fracture conductivity retention compared to conventional resin-coated sands.

Furthermore, the flexible yet robust polyurethane–nanofiller matrix may better accommodate stress fluctuations, thereby minimizing proppant flowback and structural degradation. With further refinement of coating uniformity and production scalability, this approach could present a cost-effective alternative to high-density ceramic proppants. Nevertheless, large-scale synthesis trials and long-term reservoir testing are still required to validate the coating's durability and economic feasibility for field deployment.

Abbreviations

CNT	Carbon Nanotubes
PU	Polyurethane
RCP	Resin Coated Proppant
RCS	Resin Coated Sand

References

1. Barati, R.; and Alhubail, M.M. (2020). *Unconventional hydrocarbon resources*: *Techniques for Reservoir Engineering Analysis*. John Wiley & Sons.
2. Schultz, R.; Skoumal, R.J.; Brudzinski, M.R.; Eaton, D.; Baptie, B.; and Ellsworth, W. (2020). Hydraulic fracturing-induced seismicity. *Reviews of Geophysics*, 58(3), e2019RG000695.
3. Hubbert, M.K.; and Willis, D.G. (1957). Mechanics of hydraulic fracturing. *Transactions of Society of Petroleum Engineers of AIME*, 210, 153-168.
4. Speight, J.G. (2016). *Handbook of hydraulic fracturing*. John Wiley & Sons.
5. Campos, V.P.P.D; Sansone, E.C.; and Silva, G.F.B.L.E. (2018). Hydraulic fracturing proppants. *Cerâmica*, 64(370), 219-229.
6. Liang, F.; Sayed, M.; Al-Muntasheri, G.A.; Chang, F.F.; and Li, L. (2016). A comprehensive review on proppant technologies. *Petroleum*, 2(1), 26-39.
7. Ali Hajool, Z.; Muhsan, A.S.; Al-Jothery, H.K.M.; Hamdi, S.S.; and Alakbari, F.S. (2025). Recent progress in proppant technology for improving the fracture conductivity in hydraulic fracturing. *Journal of Advanced Research Design*, 127(1), 96-119.
8. Liang, T.; Zhang, J.; Meng, C.; Xiu, N.; Cai, B.; and Fu, H. (2020). Conductivity prediction of proppant-packs based on particle size distribution under variable stress conditions. *E3S Web of Conferences*, 205, 03010.
9. Schein, G.W.; Carr, P.D.; Canan, P.A.; and Richey, R. (2004). Ultra lightweight proppants: Their use and application in the Barnett Shale, *Proceedings of the SPE Annual Technical Conference and Exhibition*, Houston, Texas, 26-19.

10. Hellmann, J.R.; Scheetz, B.E.; Luscher, W.G.; Hartwich, D.G.; and Koseski, R.P. (2014). Proppants for shale gas and oil recovery: Engineering ceramics for stimulation of unconventional energy resources. *American Ceramic Society Bulletin*, 93(1), 28-35.
11. Gu, X.; Hu, C.; Zhang, J.; and Xu, K. (2019). Laboratory tests on compaction and crushing behaviors of construction waste slag-clay mixtures. *Journal of Materials in Civil Engineering*, 31(11), 04019256.
12. Kudo, Y.; Mikami, H.; Tanaka, M.; Isaji, T.; Odaka, K.; Yamato, M.; and Kawakami, H. (2020). Mixed matrix membranes comprising a polymer of intrinsic microporosity loaded with surface-modified non-porous pearl-necklace nanoparticles. *Journal of Membrane Science*, 597, 117627.
13. Sun, Z.; Jiang, C.; Wang, X.; Zhou, W.; and Lei, Q. (2021). Combined effects of thermal perturbation and in-situ stress on heat transfer in fractured geothermal reservoirs. *Rock Mechanics and Rock Engineering*, 54(5), 2165-2181.
14. Zhao, J. et al. (2022). Ten years of gas shale fracturing in China: Review and prospect. *Natural Gas Industry B*, 9(2), 158-175.
15. He, J. (2015). *An innovative closed fracture acidizing technique for deep carbonate reservoirs using glda*. PhD Thesis, Department of Petroleum Engineering, Texas A&M University.
16. Le, V.S.; Sharma, K.V.; Hanamertani, A.S.; Youssif, M.I.; Elkhatib, O.; Rane, K.; Piri, M.; Katiyar, A.; and Nagarajan, N. (2023). Methane foam performance in oil-wet unconsolidated porous media: A systematic experimental investigation at reservoir conditions. *Fuel*, 344, 128002.
17. Zhanga, W.; Guan, X.; Fu, M.; and Zhao, S. (2018). Clay migration in proppant during production in argillaceous unconsolidated reservoir. *Aspects in Mining & Mineral Science*, 1(2), 54-57.
18. Alzanam, A.A.A.; Ishtiaq, U.; Muhsan, A.S.; and Mohamed, N.M. (2021). A multiwalled carbon nanotube-based polyurethane nanocomposite-coated sand/proppant for improved mechanical strength and flowback control in hydraulic fracturing applications. *ACS omega*, 6(32), 20768-20778.
19. Qian, T.; Muhsan, A.S.; Htwe, L.; Mohamed, N.; and Hussein, O. (2020). Urethane based nanocomposite coated proppants for improved crush resistance during hydraulic fracturing. *IOP Conference Series*: *Materials Science and Engineering*, 863(1), 012013.
20. Ishtiaq, U.; Aref, A.; Muhsan, A.S.; Rashid, A.; and Hamdi, S.S. (2022). High strength glass beads coated with CNT/rGO incorporated urethane coating for improved crush resistance for effective hydraulic fracturing. *Journal of Petroleum Exploration and Production Technology*, 12(10), 2691-2697.
21. Al-Taq, A.A.; Al-Dahlan, M.N.; and Alrustum, A.A. (2017). Maintaining injectivity of disposal wells: From water quality to formation permeability. *Proceedings of the SPE Middle East Oil & Gas Show and Conference*, Manama, Kingdom of Bahrain, D031S025R004.
22. Danso, D.K.; Negash, BM; Ahmed, T.Y.; Yekeen, N; and Ganat, T.A.O. (2021). Recent advances in multifunctional proppant technology and increased well output with micro and nano proppants. *Journal of Petroleum Science and Engineering*, 196, 108026.

23. Zhang, C.; Zhao, L.; Yu, D.; Liu, G.; Pei, Y.; Huang, F.; and Liu, B. (2019). The evaluation on physical property and fracture conductivity of a new self-generating solid proppant. *Journal of Petroleum Science and Engineering*, 177, 841-848.
24. Hajool, Z.A.; Muhsan, A.S.; Al-Jothery, H.K.M.; Nasif, M.S.; Mutaafi, A.A.; and Alakbari, F.S. (2025). Advancements in proppant coating technologies for enhanced hydraulic fracturing efficiency: A comprehensive review on nanocomposites and surface modifications. *Results in Engineering*, 28, 106179.
25. Zhang, L.; and Wang, W. (2023). Preparation and field test of double-shell coated proppant (DSCP). *Petroleum Drilling Techniques*, 51(1), 91-97.
26. Zha, C.; Green, J.; Abrams, B.; Cabori, L.; Hamori, K.; and Harper, A. (2020). On-the-fly proppant flowback control additive. *Proceedings of the SPE Annual Technical Conference and Exhibition*, Virtual, D041S056R006.
27. Ren, L.; Lin, C.; Zhao, J.; Lin, R.; Wu, J.; Wu, J.; and Hu, Z. (2024). Numerical simulation of coated proppant transport and placement in hydraulic fractures based on CFD-DEM. *Petroleum Science and Technology*, 42(22), 3334-3354.
28. Tarek, M.; and Leung, J. (2024). Novel resin-coated sand placement design guidelines for controlling proppant flowback post-slickwater hydraulic fracturing treatments. *Proceedings of the SPE Hydraulic Fracturing Technology Conference and Exhibition*, The Woodlands, Texas, USA, 29(08), 3952-3963.
29. Wang, X.; and Lin, Z. (2021) Robust, hydrophobic anti-corrosion coating prepared by PDMS modified epoxy composite with graphite nanoplatelets/nano-silica hybrid nanofillers. *Surface and Coatings Technology*, 421,127440.
30. Abdulelah, H.; Negash, B.M.; Keshavarz, A.; Hoteit, H.; and Iglauer, S. (2022). Interfacial and wetting properties in shale/methane/water and shale/methane/surfactant systems at geological conditions. *Energy & Fuels*, 36(17), 0155-10166.
31. Mora, T.; Orogbemi, O.A.; and Karpyn, Z.T. (2010). A study of hydraulic fracture conductivity and its dependence on proppant wettability. *Petroleum Science and Technology*, 28(15), 1527-1534.
32. Dong, K.; He, W.; and Wang, M. (2019). Effect of surface wettability of ceramic proppant on oil flow performance in hydraulic fractures. *Energy Science Engineering*, 7(2), 504-514.
33. Wright, A.J.; Kim, Y.; Mock, C.; Sharobem, T.; McGowan, R.; Bravo, L.; Murugan, M.; Dambra, C.; Keyes, B.; and Ghoshal, A. (2024). Influence of chemistry and surface roughness of various thermal barrier coatings on the wettability of molten sand. *Surface and Coatings Technology*, 481, 130649.
34. Krumbein, W.C.; and Sloss, L.L. (1963). *Stratigraphy and sedimentation*. (2nd ed.). W. H. Freeman and Company, San Francisco, CA.
35. Cho, G.-C.; Dodds, J.; and Santamarina, J.C. (2006). Particle shape effects on packing density, stiffness, and strength: natural and crushed sands. *Journal of Geotechnical and Geoenvironmental Engineering*, 132(5), 591-602.
36. Zhou, B.; Wang, J.; and Wang, H. (2018). Three-dimensional sphericity, roundness and fractal dimension of sand particles. *Géotechnique,* 68(1), 18-30.

37. Chen, T.; Gao, J.; Zhao, Y.; Liang, T.; Hu, G.; and Han, X. (2022). Progress of polymer application in coated proppant and ultra-low density proppant. *Polymers*, 14(24), 5534.
38. Liang, F.; Sayed, M.; Al-Muntasheri, G.A.; Chang.F.F.; Li, L. (2016) A comprehensive review on proppant technologies. *Petroleum*, 2(1), 26-39.
39. Haque, M.H.; Saini, R.K.; and Sayed, M.A. (2019). Nano-composite resin coated proppant for hydraulic fracturing. *Proceedings of the Offshore Technology Conference*, Houston, Texas, D021S021R005.
40. Pangilinan, K.D.; Al Christopher, C.; and Advincula, R.C. (2016). Polymers for proppants used in hydraulic fracturing. *Journal of Petroleum Science and Engineering*, 145, 154-160.
41. Michael, F.M.; Krishnan, M.R.; Li, W.; and Alsharaeh, E.H. (2020). A review on polymer-nanofiller composites in developing coated sand proppants for hydraulic fracturing. *Journal of Natural Gas Science and Engineering*, 83, 103553.
42. Krishnan, M.R.; Omar, H.; Aldawsari, Y.; Zien, B.A.S.; Kattash, T.; Li, W.; and Alsharaeh, E.H. (2022). Insight into thermo-mechanical enhancement of polymer nanocomposites coated microsand proppants for hydraulic fracturing. *Heliyon*, 8(12), e12282.
43. Ko, S.; Ghassemi, A.; and Uddenberg, M. (2023). Selection and testing of proppants for EGS. *Proceedings of the* 48th *Workshop on Geothermal Reservoir Engineering Stanford University*, Stanford, California, 1-12.